Extended Abstracts of the 2009 International Conference on Solid State Devices and Materials, Sendai, 2009, pp480-481

# Enhanced Photovoltaic Effects of InGaN-based Materials for Future Full-Solar-Spectrum Solar Cells

Chih-Ciao Yang[1], Jinn-Kong Sheu[1], Shang-Ju Tu[1], Chun-Kai Tseng[1], Min-Shun Huang[1], Kuo-Hua Chang[1], Tao-Hung Hsueh[1], Ming-Lun Lee[2], Li-Chi Peng[1], and Wei-Chih Lai[1]

[1]Institute of Electro-Optical Science and Engineering, National Cheng Kung University, Tainan City 70101, Taiwan
Phone: +886-6-2757575ext65298ext103 E-mail: papilionidae@gmail.com
[2]Department of Electro-Optical Engineering, Southern Taiwan University, Tainan 71005, Taiwan

## 1. Introduction

Group III-nitride compound semiconductors of the $In_XGa_{1-X}N$ alloy system providing full-solar-spectrum photovoltaic (PV) applications has been predicted since 2002 by the bandgap confirmation of InN [1-2]. Applying the $In_XGa_{1-X}N$ alloy system, the photon energy within the solar spectrum, especially in the visible and infrared regions where yield the most solar energy conversion, is continuously available for the PV fabrication between 0.7 eV (InN) of infrared and 3.4 eV (GaN) of ultraviolet regions. Recently because of the potential multi-junction solar cells for the ultra-high conversion efficiency over 50%, several groups have reported their efforts in the research of the InGaN-based PV devices [3-6]. However, the present InGaN-based materials exhibit much more difficulty in the epitaxy growth than conventional GaAs or Si semiconductors, mainly due to material qualities such as the uniformity, compound miscibility from different optima growth temperature of InN (~700℃) and GaN (~1000℃), phase separation and natural structure defects from mismatched substrates. These factors may seriously influence the PV effects for InGaN-based PV devices. It is still a great challenge to lower down the bandgap energy of InGaN that the material quality degrades rapidly with the increase of the indium content and thickness in the InGaN alloys. Therefore, some fundamental studies for InGaN-based PV devices are necessary to clarify before the full-solar-spectrum PV device is realized.

## 2. Experiments and Results

Samples used in this study were grown on c-face sapphire substrates. The p-i-n structure consisted of a 1-μm-thick unintentionally GaN layer, a 2.3-μm-thick Si-doped $n^+$-GaN followed by an unintentionally doped 200-nm-thick InGaN/GaN-based active layer, and a 60-nm-thick Mg-doped p-InGaN top layer grown at 750 °C. The carrier concentration of the $n^+$-GaN and the p-$In_{0.19}Ga_{0.81}N$ layers were around $5\times10^{18}$ and $1\times10^{18}$ $cm^{-3}$, respectively. The active i-layer was an $In_{0.25}Ga_{0.75}N$/GaN superlattice structure consisting of 28 pairs, where the GaN barrier layers and the InGaN well layers were 4 nm and 3 nm, respectively [6]. The fabrication process is similar to present GaN-based light-emitting diodes (LEDs). During the fabrication processes, the inductively-coupled plasma (ICP) dry etching was applied to expose the underlying $n^+$-GaN for the formation of Ohmic contacts. The transparent conducting layer of indium tin oxide (ITO) was deposited onto the p-InGaN top layer by the electron beam evaporator. Finally, the Cr/Au (50/1000 nm) bi-layer metal was deposited on the exposed $n^+$-GaN surface and the ITO layer to serve as the cathode and the anode electrodes at the same time. The fabricated device is shown in figure 1.

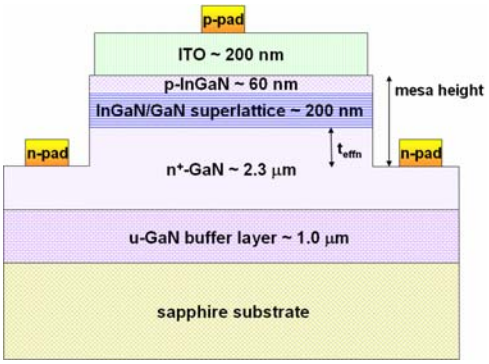


Fig. 1 The fabricated device with digitated pad deploys and different mesa height.

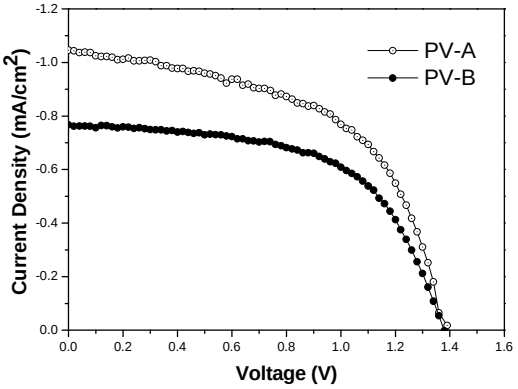


Fig. 2 J-V characteristics under AM1.5G irradiance of different $t_{effn}$ for PV-A with 40 nm and PV-B with 740 nm.

In order to realize how high resistivity InGaN materials affect the current collection under solar irradiance, we provided digitated deploys for electrode pads with two mesa height of 300 and 1000 nm, labeled as PV-A and PV-B, respectively. Figure 2 shows the characteristics between current density and voltage (J-V) taken from the PV devices illuminated by the Oriel solar simulator (model: M-91190A) which was calibrated by the calibration cell of NREL under well known AM1.5G conditions. Although the open-circuit voltage ($V_{OC}$) of PV-A is slightly larger than that of PV-B (both $V_{OC}$ ~ 1.4 V), the short-circuit current density ($J_{SC}$) of PV-A is 1.05 mA/$cm^2$, which is about

35% enhancement more than that of PV-B (~0.78 mA/cm$^2$). Here, no antireflection coatings were applied. The series resistance, which is extracted from the method of multi-sun illuminations [7], of PV-A and PV-B are 29.6 and 74.0 Ω, respectively. As a result, the effective thickness ($t_{effn}$) vertically from the absorption layer to n-electrode is 40 nm and 740 nm for PV-A and PV-B, respectively. That is to say, the high resistivity of GaN materials and high defect (dislocation density usually $10^9$~$10^{10}$ cm$^{-2}$ in GaN/sapphire-based epitaxy) both dominate the current collection efficiency in InGaN-based PV devices. Especially when the InGaN layer is thick, the high-defect-density materials tend to capture the light-induced carriers, and limit the carrier transport length [8-10].

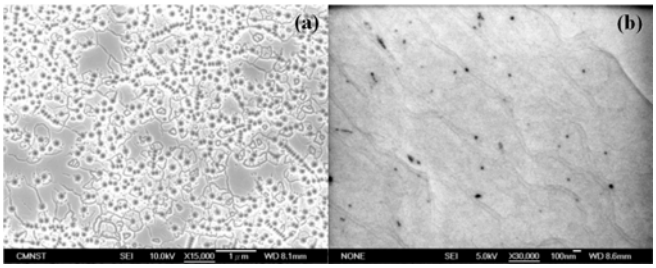


Fig. 3 (a) The surface conditions of SEM images for PV-C with a 200 nm GaN/InGaN superlattice absorption layer and (b) PV-D with only half the absorption thickness.

Table I. The PV effect of average enhancement in percentage (%) for PV-C and PV-D after depositing $SiO_2$ films onto the devices.

| | $V_{oc}$ | $J_{sc}$ | FF | Efficiency |
|---|---|---|---|---|
| PV-C | **absent** | **10.9** | **0.9** | **10.9** |
| PV-D | **9.1** | **11.4** | **5.2** | **26.9** |

Since the InGaN-based materials have large defect density, we performed post-treatment to alleviate the treading dislocations (TDs) resulting from mismatched substrates and the thick 28-pair superlattice structure with a 200-nm-thick absorption layer. Here the high transparency and stability silicon dioxide ($SiO_2$) coating was used to passivate the surface defects. The $SiO_2$ film was deposited by plasma-enhanced chemical vapor deposition (PECVD), and its thickness was adjusted to reduce the Fresnel reflection loss of incident light at the same time. The test cells with $SiO_2$ coatings onto aforementioned devices with a 300-nm-thick mesa are labeled as PV-C. Besides, we also performed another 14-pair superlattice structure with a 100-nm-thick absorption layer, which is only half the absorption thickness that discussed above, and the fabricated process was the same as PV-C, labeled as PV-D. Figure 3(a) and 3(b) shows the images of top surface conditions performed by scanning-electron-microscopy (SEM) for PV-C (15,000X) and PV-D (30,000X), respectively. The top surface crack with diameter greater than 100 nm is around $2.5\times10^{10}$ and $4.3\times10^{6}$ cm$^{-2}$ for PV-C and PV-D, respectively. These dense surface defects could be attached to the underlying threading dislocations, which mainly arise from the large lattice mismatch within the thick InGaN/GaN superlattice and the mismatched sapphire substrates. Table I shows the average enhancement in percentage (%) after the $SiO_2$ passivation coating layer is deposited onto the devices. Although $J_{SC}$ of both PV-C and PV-D is enhanced for about 11% due to the reduction of Fresnel reflection loss, the $V_{OC}$ enhancement of PV-C is less obvious than PV-D (~9.1%). This is because the surface recombination of PV-C is much serious than PV-D, which has fewer (~1/10000) surface cracks. As a result, the $SiO_2$ coatings could passivate the defect more efficiently in PV-D. However, PV-C with large InGaN/GaN superlattice of 200 nm could induce more current leakage paths from treading dislocations and thereby lower down the shunt resistance in the PV devices. As a result, the measured $V_{OC}$ is far less than the predicted value, which is in principle close to the bandgap of absorption layers.

## 3. Conclusions

Although the conversion efficiency is still low in InGaN-based PV devices, the dominant factor is the material quality of the InGaN semiconductors. Methods to enhance the epitaxy quality have been still challenging and very expensive to date. In this study, we provide that the shallower mesa device with $t_{effn}$ of 40 nm has 35% more enhancement than that with $t_{effn}$ of 740 nm in the current collection. The post-treatment of $SiO_2$ passivation coatings enhance 9.1% in $V_{OC}$ when the defect density is less serious.


## Acknowledgements

This work has been granted by Frontier Materials and Micro/Nano Science and Technology Center, NCKU. The authors would also like to acknowledge the National Science Council for the financial support and provision of the research grant NSC 97-2221-E-006-242-MY3.


## References


[1] Y. Davydov, A. A. Klochikhin, R. P. Seisyan, V. V. Emtsev, S. V. Ivanov, F. Bechstedt, J. Furthmuller, H. Harima, A. V. Mudryi, J. Aderhold, O. Semchinova, and J. Graul, Phys. Status Solidi B **229** (2002) R1.

[2] J. Wu, W. Walukiewicz, K. M. Yu, J. W. Ager III, E. E. Haller, Hai Lu, William J. Schaff, Yoshiki Saito, and Yasushi Nanishi, Appl. Phys. Lett. **80** (2002) 3967.

[3] O. Jani, I. Ferguson, C. Honsberg and S. Kurtz, Appl. Phys. Lett. **91** (2007) 132117.

[4] C. J. Neufeld, N. G. Toledo, S. C. Cruz, M. Iza, S. P. Denbaars and U. K. Mishra, Appl. Phys. Lett. **93** (2008) 143502.

[5] X. Zheng, R. H. Horng, D. S. Wuu, M. T. Chu, W. Y. Liao, M. H. Wu, R. M. Lin and Y. C. Lu, Appl. Phys. Lett. **93** (2008) 261108.

[6] J. K. Sheu, C. C. Yang, S. J. Tu, K. H. Chang, M. L. Lee, W. C. Lai and L. C. Peng, IEEE Electron Device Lett. **30** (2009) 3.

[7] Dieter K. Schroder, Semiconductor Material and Device Characterization, 3rd edition (2005).

[8] I.-H. Kim, H.-S. Park, Y.-J. Park, and T. Kim, Appl. Phys. Lett. **73** (1998) 1634.

[9] M. J. Reed, N. A. El-Masry, C. A. Parker, J. C. Roberts, and S. M. Bedair, Appl. Phys. Lett. **77** (2000) 4121.

[10]D. Holec, P.M.F.J. Costa, M.J. Kappers, and C.J. Humphreys, J. Crystal Growth **303** (2007) 314.